Heliyon

Received:
31 May 2017
Revised:
29 September 2017
Accepted:
13 November 2017

Cite as:
Miguel Ángel López Zavala, Samuel Alejandro Lozano Morales, Manuel Ávila-Santos. Synthesis of stable TiO_2 nanotubes: effect of hydrothermal treatment, acid washing and annealing temperature.
Heliyon 3 (2017) e00456.
doi: 10.1016/j.heliyon.2017.e00456

Synthesis of stable TiO_2 nanotubes: effect of hydrothermal treatment, acid washing and annealing temperature

Miguel Ángel López Zavala [a,*], **Samuel Alejandro Lozano Morales** [b,c], **Manuel Ávila-Santos** [c]

[a] *Tecnológico de Monterrey, Water Center for Latin America and the Caribbean, Av. Eugenio Garza Sada Sur No. 2501, Col. Tecnológico, Monterrey, N. L., México, C.P. 64849*

[b] *Cátedra CONACYT, Centro de Química, Instituto de Ciencias, Universidad Autónoma de Puebla, Ciudad Universitaria, Edif. 103H, Puebla, Pue. 72570, México*

[c] *Instituto Politécnico Nacional, CICATA-Legaría, México D.F., México*

* Corresponding author.

E-mail address: miganloza@itesm.mx (M.Á. López Zavala).

Abstract

Effect of hydrothermal treatment, acid washing and annealing temperature on the structure and morphology of TiO_2 nanotubes during the formation process was assessed. X-ray diffraction, scanning electron microscopy (SEM), transmission electron microscopy (TEM) and energy dispersive X-ray spectroscopy analysis were conducted to describe the formation and characterization of the structure and morphology of nanotubes. Hydrothermal treatment of TiO_2 precursor nanoparticles and acid washing are fundamental to form and define the nanotubes structure. Hydrothermal treatment causes a change in the crystallinity of the precursor nanoparticles from anatase phase to a monoclinic phase, which characterizes the TiO_2 nanosheets structure. The acid washing promotes the formation of high purity nanotubes due to Na^+ is exchanged from the titanate structure to the hydrochloric acid (HCl) solution. The annealing temperature affects the dimensions, structure and the morphology of the nanotubes. Annealing temperatures in the range of 400

http://dx.doi.org/10.1016/j.heliyon.2017.e00456

°C and 600 °C are optimum to maintain a highly stable tubular morphology of nanotubes. Additionally, nanotubes conserve the physicochemical properties of the precursor Degussa P25 nanoparticles. Temperatures greater than 600 °C alter the morphology of nanotubes from tubular to an irregular structure of nanoparticles, which are bigger than those of the precursor material, i.e., the crystallinity turn from anatase phase to rutile phase inducing the collapse of the nanotubes.

Keywords: Nanotechnology, Materials science

1. Introduction

Recently, advanced oxidation processes such as photocatalysis have been proposed to degrade emergent contaminants. Photocatalysis is an energy efficient, harmless and sustainable process that has called the interest for practical applications. Among several catalysts, the TiO_2 has been widely studied and it is commonly used in industry due to its photoactivity efficiency, stability, and cost [1, 2]. Nanostructures of TiO_2 such as nanotubes, nanocables, and nanobelts have been recognized as great catalysts by several researchers [3, 4, 5]. Specially, photocatalytic activity, ion-exchange capacity, high surface area and structure with layered walls are interesting physicochemical properties of TiO_2 nanotubes [1]. High surface area of nanotubes improves the electron transfer and consequently their efficiency on different applications. Characteristics such as high purity, crystallinity, and stability at high temperatures are required by such applications [6]. Different processes such as sol-gel [7], anodization [8], and molecular assembly [9] have been used to synthesize TiO_2 nanotubes; however, these techniques cannot produce low dimensional TiO_2 nanotubes with high crystallinity. Better results have been obtained with the application of a hydrothermal method commonly used to prepare zeolite catalysts on an industrial scale; it is a simple synthesis method, where the products properties depend on the formation mechanism and hydrothermal parameters. Formation of TiO_2 nanotubes is influenced by the synthesis conditions (TiO_2 precursor, temperature, pressure and reaction time), and the use of auxiliary techniques; such as: ultrasonication, microwave, acid washing and calcination [1]. A cheap and safety alkaline hydrothermal technique was introduced by Kasuga et al. to synthesize nanotubes with high purity [10, 11]. They found that formation of nanotubes of TiO_2 depends on the hydrothermal treatment and the purification process; but they did not discuss the effect of the annealing temperature on the thermal stability, morphology and crystalline structure of nanotubes and the influence of these properties on the photocatalytic effect.

The annealing temperature is the main parameter that affects the formation of TiO_2 nanotubes according to Wang et al. [12], Kiatkittipong et al. [13] and B. Vijayan et al. [14], but in their reports, they did not discuss about the morphology and

http://dx.doi.org/10.1016/j.heliyon.2017.e00456

crystallinity of nanotubes. Despite several researches conducted on hydrothermal synthesis and formation mechanism of TiO_2 nanotubes since 1998 [1], there are still debate related to the formation mechanism and the crystalline structure of nanotubes. The extremely small size of the tubular structures hinders direct experimental measurements to confirm the proposed formation mechanisms. Mohsen et al., report a method to fabricate an effective, reproducible, and inexpensive visible-light-driven photocatalyst for environmental applications [15].

Thus, paper investigates the synthesis of stable TiO_2 nanotubes, the effect of the hydrothermal treatment, HCl-washing, and the annealing temperature on the formation process, structure, and morphology of TiO_2 nanotubes.

2. Materials and methods

2.1. Chemical reagents for the synthesis of TiO_2 nanotubes

All chemical reagents used in this study were analytical grade (Table 1). For the synthesis of TiO_2 nanotubes, Degussa P25 (88% anatase and 12% rutile) was used as a precursor from Aeroxide (Evonik, Germany). Sodium hydroxide (NaOH) and hydrochloric acid (HCl) were purchased form J.T. Baker (Center Valley, PA, USA). Ultra-pure water was prepared with a Milli-Q water purification system (Bedford, MA, USA).

2.2. Synthesis of TiO_2 nanotubes

TiO_2 nanotubes were synthesized using a procedure similar to that described by Kasuga et al. [10]. 0.3 g of Degussa P25 TiO_2 nanoparticles were dispersed into 30 ml of a 10 M sodium hydroxide solution. The suspension was stirred vigorously for 2 hours at 30 °C. Then, the suspension was autoclaved at 110 °C for 72 h. The product obtained was redispersed in 200 ml of a 0.1 M HCl solution for 3 hours [16] (See Fig. 1). Then, the suspension was centrifuged and the solid sample was washed with distilled water until pH was stabilized at 6.7. Finally, the sample was dried at 80 °C for 24 h in a vacuum oven. The dried sample was divided into three portions and then annealed at 400 °C, 600 °C and 800 °C for 2 hours, respectively.

Table 1. Physical properties of the chemical reagents.

Reagent	Formula	Molecular Weight (g/mol)	Purity (%)
Degussa P25	TiO_2	79.87	≥99.5
Sodium Hydroxide	NaOH	40	99.1
Hydrochloric acid	HCl	36.46	99.7
Distilled water	H_2O	18.01	18 Ω

http://dx.doi.org/10.1016/j.heliyon.2017.e00456

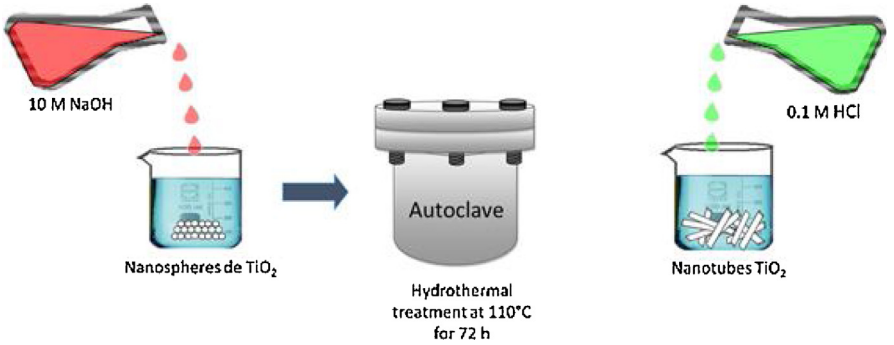

Fig. 1. Hydrothermal synthesis of TiO_2 nanotubes.

2.3. Structural and morphological characterization of TiO_2 nanotubes

Annealed samples were powdered by using an agate mortar and then analyzed. Structural characterization of nanotubes was performed by X-ray diffraction (XRD). A Bruker AXS-D5000 diffractometer was used with a Cu Kα wavelength (λ = 1.5418 Å), diffraction angle (2θ) ranging from 5° to 90°, step size of 0.020°, scan speed of 0.6 s/step and a temperature of 300 K.

Average size, composition and morphology of nanotubes were examined using a JEM-2100 (JEOL) transmission electron microscope (TEM). The samples were placed in a sample holder and analyzed by energy-dispersive spectroscopy (EDS). The operation conditions were: accelerating voltage, 15 eV; current, 75 mA; pressure, 1.3×10^{-3} Pa; and working distance, 25 mm. Additionally, Varian, Cary-100 scan spectrophotometer was used for evaluating the band-gap values of synthesized TiO_2 nanotubes. The optical band-gap energy of TiO_2 nanotubes was obtained from UV–vis reflectance spectra.

3. Results and discussion

3.1. Structural characteristics of TiO_2 nanotubes

Fig. 2 shows the X-ray diffractograms of nanotubes after different treatments. (a) represents the precursor Degussa P25; (b) nanostructures after hydrothermal treatment at 110 °C; (c) annealed nanotubes after acid washing with 0.1 M HCl solution; (d, e, f) nanotubes after annealing treatment in air for 2 h at 400 °C, 600 °C, and 800 °C., respectively. The annealing treatment was conducted to observe the thermal stability of the nanotubes. Crystalline phases present in nanotubes were identified using the X-ray diffractograms obtained and by profile fitting using the PDF-2 database from the International Center for Diffraction Data. The profile fitting was conducted following the Le Bail method [17] and using the FULLPROF software [18]. The average size of nanoparticles was estimated using the Scherrer equation (Eq. (1)).

http://dx.doi.org/10.1016/j.heliyon.2017.e00456

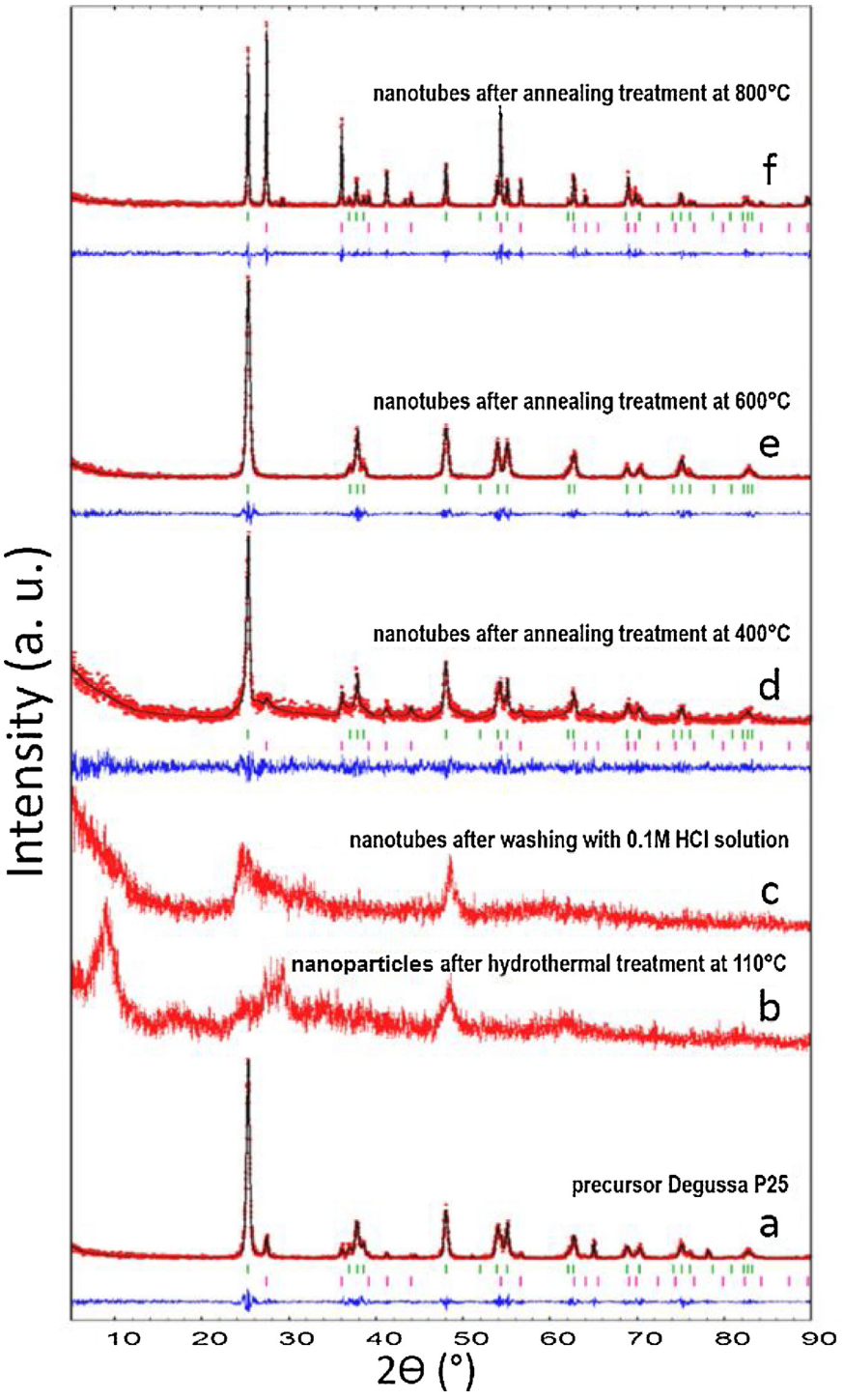

Fig. 2. X-ray diffractograms of nanotubes after different hydrothermal treatments. (a) represents the precursor Degussa P25; (b) nanostructures after hydrothermal treatment at 110 °C; (c) annealed nanotubes after acid washing with 0.1 M HCl solution; (d) nanotubes after annealing treatment at 400 °C; (e) nanotubes after annealing treatment at 600 °C; (f) nanotubes after annealing treatment at 800 °C in air for 2 h. In red experimental pattern; in black calculated pattern, based on the Le Bail method; and in blue the profile fitting difference. Green vertical bars correspond to the Bragg positions of anatase

http://dx.doi.org/10.1016/j.heliyon.2017.e00456

$$L = \frac{K\lambda}{\beta\cos\theta} \quad (1)$$

where L is the estimated nanocrystallite size; K is the shape factor, in this case was taken as 0.89; λ is the wavelength of X-ray diffraction radiation in nm; β is the peak width of the diffraction peak profile at the half maximum height resulting from small crystallite size; and θ is the diffraction angle.

From X-ray diffractograms (Fig. 2, profile (a)), anatase and rutile phases of the Degussa P25 precursor were identified. Le Bail profile fitting reveled an 88% of anatase and 12% of rutile phases. The profile difference (in blue) indicated a good fitting between the calculated and experimental profiles. The estimated average crystallite size was 24 nm, which corresponds to the values reported by the precursoŕs manufacturer.

The profile (b) corresponds to the nanotubes structure after the hydrothermal treatment at 110 °C; as seen, good fitting to the $Na_2Ti_3O_7$ monoclinic phase (JCPDS 00-059-0666) [21] was observed. Three main peaks located at 9.6°, 25.1° and 29.5° were identified. Additionally, the experimental profile also presented an important peak at 48.4°, which might suggest that anatase structure of the precursor nanoparticles were present in minor quantity. Due to the low crystallinity of the sample, the Le Bail profile fitting could not be determined.

$Na_2Ti_3O_7$ is a layered compound, reported by [22], which is synthesized through the reaction in Eq. (2).

$$3TiO_2 + 2NaOH \rightarrow Na_2Ti_3O_7 + H_2O \quad (2)$$

Through the hydrothermal treatment, shown in reaction (2), some of the Ti–O–Ti bonds of the TiO_2 precursor break and a six-coordinated monomer $[Ti(OH)_6]_2$ is formed and saturated. This monomer is unstable and combines by oxolation or olation to form nuclei. They become thermodynamically stable when grow and their size exceeds the critical nuclei size [23]. During the growing process, thin nanosheets can be formed and integrated of layer unit cells. The growth of these nanosheets is anisotropic, being the growth along the b-axis the fastest, which leads to the formation of 1D $Na_2Ti_3O_7$ nanostructures. The crystal structure of $Na_2Ti_3O_7$ is monoclinic with layers of $[TiO_6]$ octahedral sites with shared edges and vertices, and with Na^+ cations located between the $[TiO_6]$ layers. The synthesis of $Na_2Ti_3O_7$ nanotubes occurs at lower temperatures; where the hydrogen deficiency in the surface of the nanosheets increment the surface tension and the tendency of the surface layer to bend. The surface strain energy becomes larger due to the increase of hydrogen-deficient sites to the point that the surface layer can overcome coupling between layers and exfoliate off from the layer underneath [24].

phase (JCPDS 01-089-4921) [19], while red vertical bars correspond to rutile phase (JCPDS 01-086-0148) [20].

http://dx.doi.org/10.1016/j.heliyon.2017.e00456

The $Na_2Ti_3O_7$ conversion to $H_2Ti_3O_7$, which is a related structure, requires an ion exchange process. When $Na_2Ti_3O^7$ is immersed and washed with diluted hydrochloric acid solution, the Na^+ ions in the TiO_2 matrix are replaced by H_3O^+ ions to form $H_2Ti_3O_7$, as shown in Eq. (3).

$$Na_2Ti_3O_7 + 2HCl \rightarrow H_2Ti_3O_7 + 2NaCl \quad (3)$$

In Eq. (3), anatase structure may be obtained by annealing the $H_2Ti_3O_7$ at 700 °C for 2 h [25], through crystal lattice rearrangement as given by Eq. (4).

$$H_2Ti_3O_7 \rightarrow 3TiO_2 + H_2O \quad (4)$$

The profile (c) in Fig. 2 presents two peaks located at 25.3° and 48.1°. These peaks have a good fitting with the anatase phase (JCPDS 01-089-4921) [19]; however, the profile fitting could not be determined due to the low crystallinity of the sample. Several researches [26, 27, 28, 29] attribute this fact to the collapse of the nanotubes due to the exchange of Na^+ ions present in the nanotubes structure; however, in this study, instead of collapse of the nanotubes, nanosheets formation as a precursor of the nanotubes was the reason of the low crystallinity observed at this stage of the synthesis.

The profile (d) reveals that both anatase and rutile phases were present in this sample. The main phase was anatase with 72%, while rutile represented 28%. These results suggest that nanotubes annealed at 400 °C recovered the anatase structure of the precursor nanoparticles.

The profile (e) presented 100% of anatase phase, accordingly to profile fitting pattern. This indicates that the anatase structure of nanotubes of sample (d)

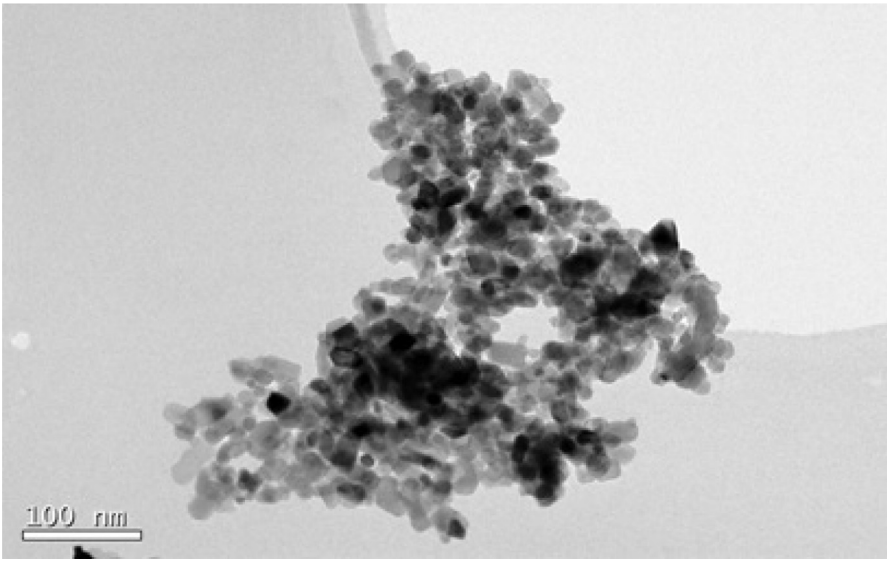

Fig. 3. TEM image of TiO_2 precursor nanoparticles (Degussa P25).

http://dx.doi.org/10.1016/j.heliyon.2017.e00456

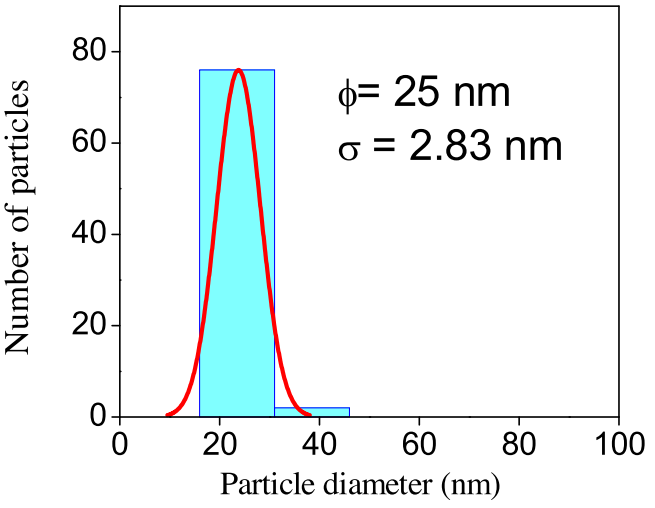

Fig. 4. Average size of TiO_2 nanoparticles (Degussa P25).

improved as the annealing temperature increased from 400 °C to 600 °C. On the contrary, at 800 °C the XRD pattern (Fig. 2, profile (f)) reveals that the anatase phase changed to rutile phase. Le Bail profile fitting showed a phases distribution of 40% for anatase and 60% for rutile. TEM images reveals that nanotubes were destroyed and converted into non-uniform nanoparticles at annealing temperatures greater than 600 °C, as discussed in section 3.2.

3.2. Morphology of TiO_2 nanotubes

Fig. 3 shows a TEM micrograph of TiO_2 precursor nanoparticles (Degussa P25). As seen, nanoparticles are not uniform. According to the histogram (Fig. 4) the

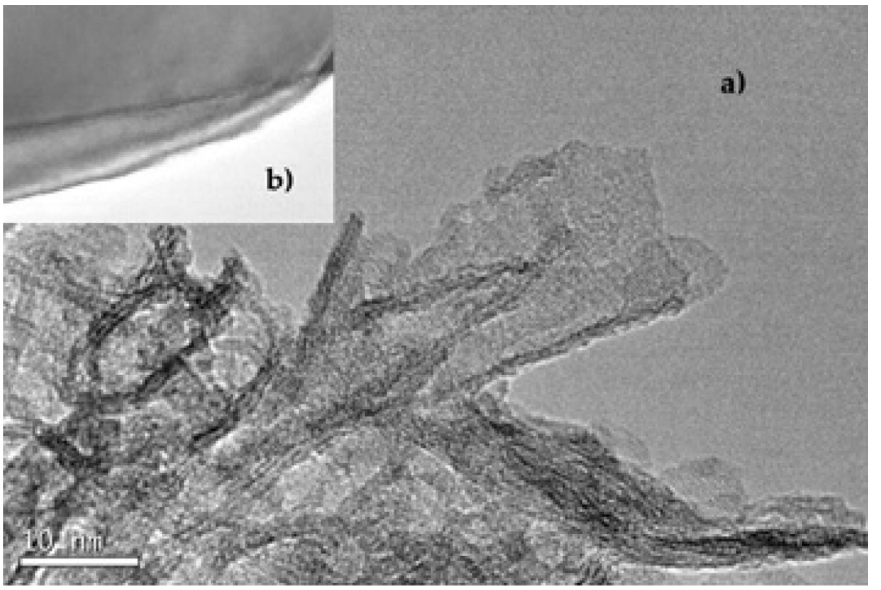

Fig. 5. TEM micrographs of precursor nanoparticles after hydrothermal treatment: (a) nanosheets formation, (b) curled end of the nanosheets.

http://dx.doi.org/10.1016/j.heliyon.2017.e00456

average size was 25 nm with a standard deviation of 2.83 nm. This result is similar to that obtained with Eq. (1).

Fig. 5 shows TEM micrographs of the precursor nanoparticles after the hydrothermal treatment at 110 °C and 72 h reaction time, prior to the acid washing process. As seen, no tubular structures or particles were identified, but nanosheets structures were clearly observed. According to the formation mechanism [30], if the tubular structure has been formed, a couple of walls of multiple layers would be observed [31, 32]. In Fig. 5, the formation of nanosheets (2D) with a random distribution and a nearly curled end was observed. These results differed from those of the literature that reports that nanosheets are formed in reaction times lower than 72 h [10, 11, 28, 33, 34, 35]. According to the formation mechanism of TiO_2 nanotubes proposed by [30], 2D nanosheets constitute an intermediate step, essential to the formation of nanotubes [36].

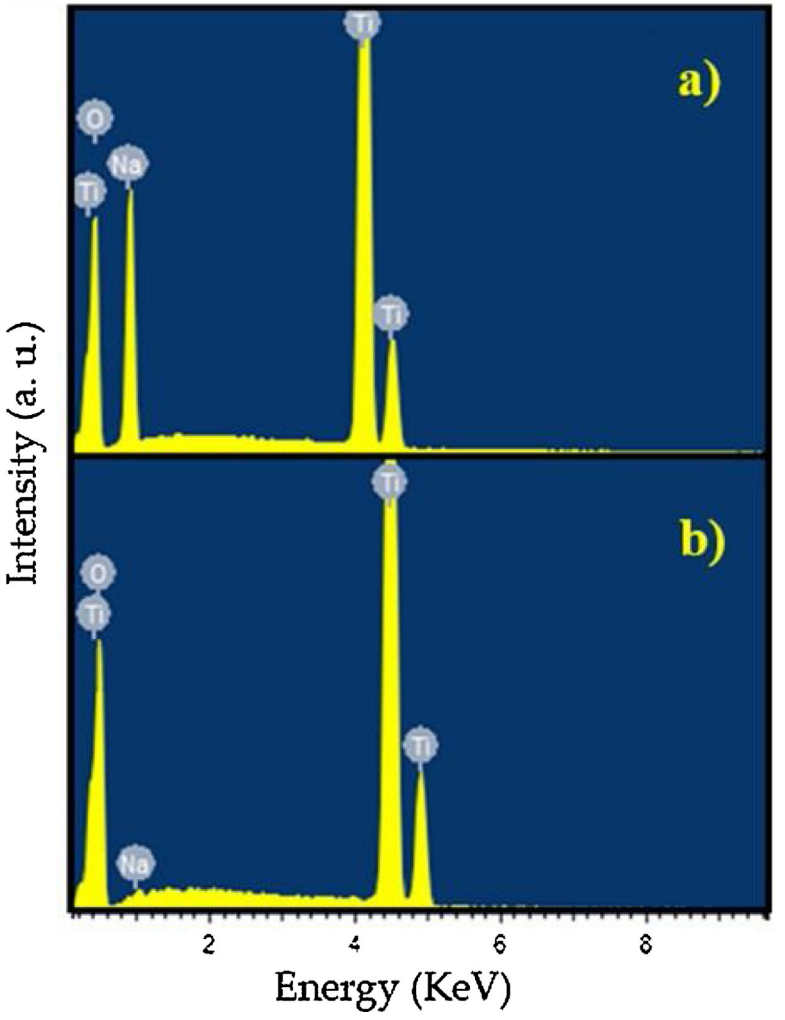

Fig. 6. EDS spectra of nanotubes (a) after hydrothermal treatment without acid washing process, (b) after acid washing process.

http://dx.doi.org/10.1016/j.heliyon.2017.e00456

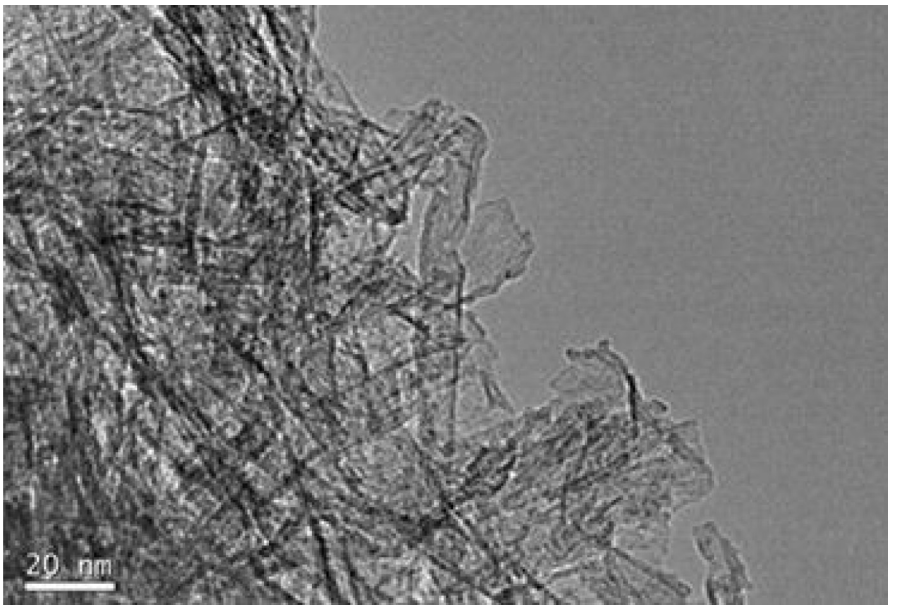

Fig. 7. TEM micrograph of nanotubes formation, after the hydrothermal treatment at 110 °C and the acid washing process with 0.1 M HCl solution.

Wang et al. [30] found that the acid washing process and the acidity of the solution determine the morphology, length and other properties of nanotubes such as composition, annealing characteristics, and specific surface. In this research, the acid washing process with 0.1 M HCl solution altered the intensities of the peaks in the XRD pattern (Fig. 2c) due to changes in the titanate structure. These changes occurred because the nanotubes exchanged Na^+ ions to the HCl solution as observed in the EDS results (Fig. 6). These results are in accordance with those reported by [37] who considered that the acid washing process is required for the formation of high purity nanotubes. Thus, the acid washing process influences the formation of nanotubes and the hydrothermal treatment affect their structural composition [12].

Formation of nanotubes after the acid washing process was observed from TEM results (Fig. 7). From the histogram (Fig. 8) the average inner diameter was determined as 7.5 nm, the external diameter as 8.4 nm and the length as 34 nm.

Fig. 9 presents the results of the TEM and SEM analysis of nanotubes after the annealing treatment at 400 °C and 600 °C. As seen, the tubular morphology did not change in both temperatures. According to the histogram shown in Fig. 10 (a), the characteristics of the nanotubes annealed at 400 °C were, inner diameter: 7.2 nm, outer diameter: 8.1 nm, length: 20–30 nm. This result was similar to that calculated from XRD analysis in Fig. 2, profile (d). On the other hand, the dimensions of nanotubes annealed at 600 °C (Fig. 10b) were, inner diameter: 7.1 nm, outer diameter: 8.1 nm, length: 28 nm. As shown in Fig. 9 (b and d), not only the tubular

http://dx.doi.org/10.1016/j.heliyon.2017.e00456

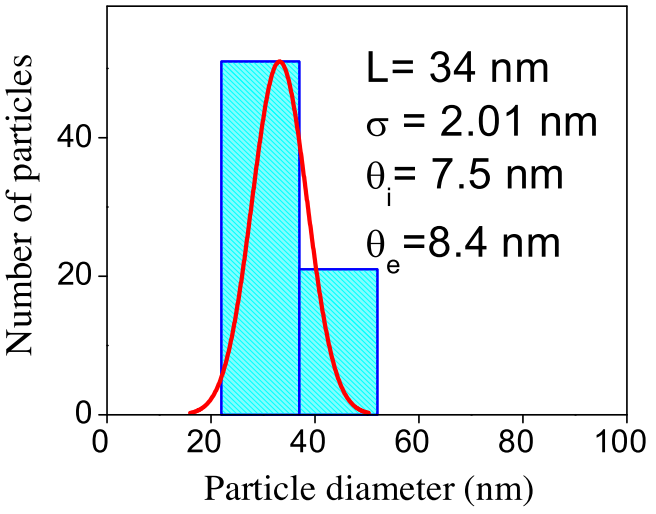

Fig. 8. Average size distribution of nanotubes after the acid washing process.

morphology was maintained, but also, the dimensions were quite similar, denoting the stability of nanotubes when they are subjected to this range of annealing temperatures. The tubular morphology is proved observing the SEM images for each annealing temperature.

When the nanotubes were annealed at 800 °C, their crystalline structure changed from complete anatase phase at 600 °C to an structure composed of anatase (40%)

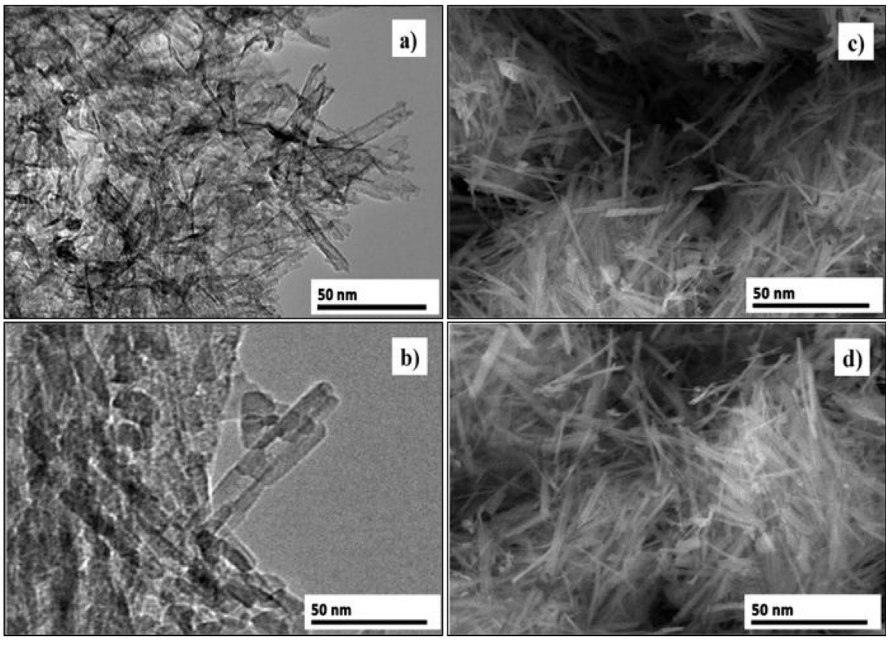

Fig. 9. TEM and SEM images of TiO_2 nanotubes annealed at 400 °C (a) and c), respectively) and 600 °C (b) and d), respectively).

http://dx.doi.org/10.1016/j.heliyon.2017.e00456

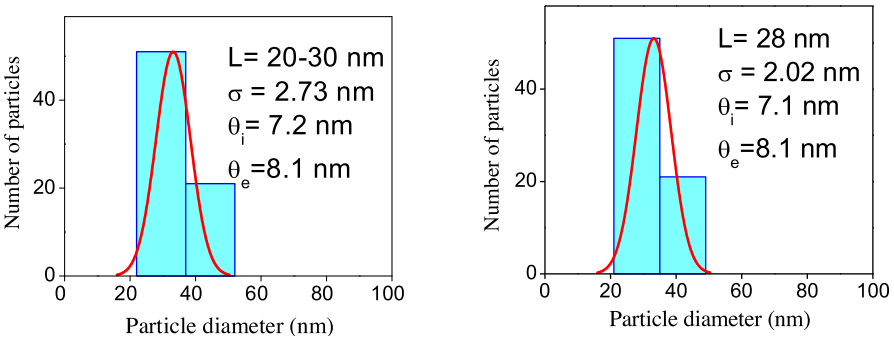

Fig. 10. Average size distribution of nanotubes annealed at 400 °C (a) and 600 °C (b).

and rutile (60%) phases, as stated in Section 3.1 (Fig. 2, profile (f)). This change was confirmed by the TEM image shown in Fig. 11. As seen, nanotubes morphology disappeared to form nanoparticles with average diameter of 116 nm (Fig. 12), greater than that of the precursor material. Similar results are reported by [38]. They observed that high annealing temperature contributes to the collapse of nanotubes due to the evaporation of hydroxyl groups. Reduction of the number of hydrogen bonds causes the destruction of nanotubes, forming nanoparticles with large dimensions.

DRS spectra of the nanotubes annealed at 400 °C is presented in Fig. 13. The band gap energy (Eg) of the nanotubes sample was estimated using the Kubelka–Munk model and by plotting a line from the maximum slope of the curve to the x-axis.

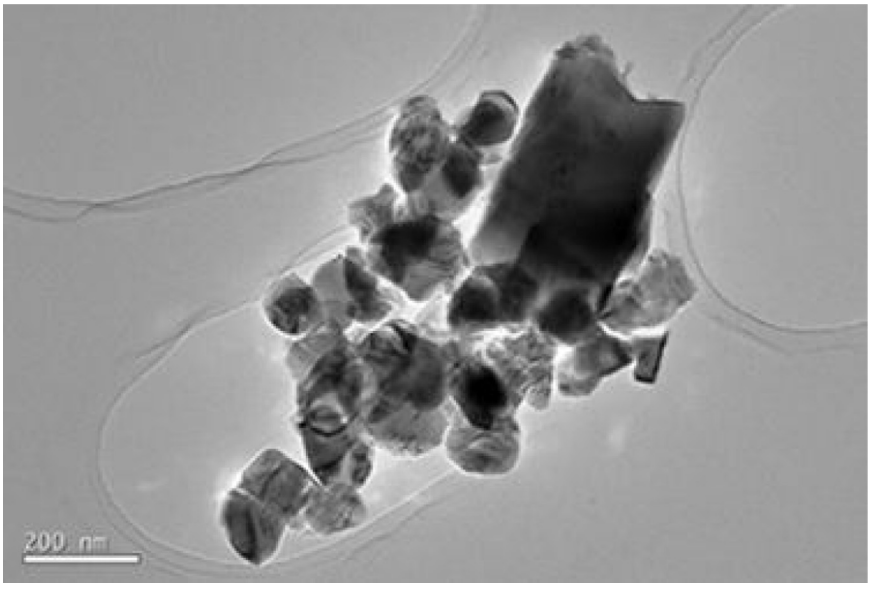

Fig. 11. TEM micrographs. Nanoparticles formed after annealing nanotubes at 800 °C.

http://dx.doi.org/10.1016/j.heliyon.2017.e00456

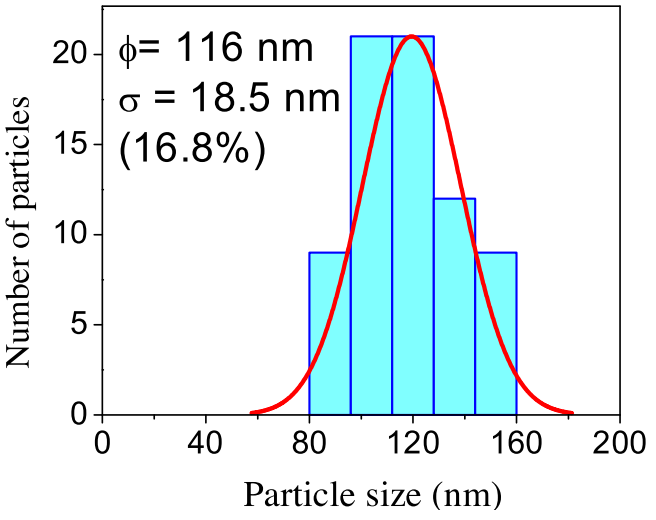

Fig. 12. Average size distribution of nanoparticles formed after annealing nanotubes at 800 °C.

The absorption was found to be 378 nm and the band gap energy of Eg = 3.28 eV. The literature data concerning band gap of TiO_2 nanotubes are inconsistent, depending on the hydrothermal treatment time; but band gap values reported for anatase phase in bulk is approximately 3.2 eV [39], value quite similar to the obtained in this study. It means that physico-chemical properties of TiO_2 nanotubes are very close to the properties of TiO_2 precursor nanoparticles, i.e., nanotubes preserved the physico-chemical properties of the precursor Degussa P25 material, which is desirable.

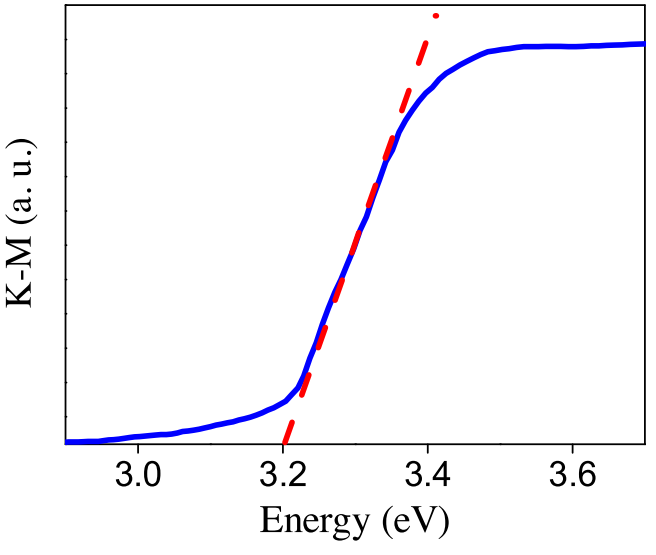

Fig. 13. UV-vis-DRS spectra of TiO_2 nanotubes annealed at 400 °C.

http://dx.doi.org/10.1016/j.heliyon.2017.e00456

Table 2. Characterization of TiO_2 nanotubes via XRD and TEM.

Figure	Treatment	Structure (XRD)	Morphology (TEM)	Average size (nm)
2a	Precursor Degussa P25	Anatase 88%, Rutile 12%	Irregular	25
2b	Hydrothermal treatment	Monoclinic	Nanosheet	30
2c	Acid washing	Anatase	Nanotube	Di = 7.5, De = 8.4, L = 34
2d	Annealing at 400 °C	Anatase 72%, Rutile 28%	Nanotube	Di = 7.2, De = 8.1, L = 20 −30
2e	Annealing at 600 °C	Anatase 100%	Nanotube	Di = 7.1, De = 8.1, L = 28
2f	Annealing at 800 °C	Anatase 40%, Rutile 60%	Irregular	116

Based on above results, Table 2 summarizes the structural and morphological characteristics of nanotubes synthetized in this research.

4. Conclusions

Effect of hydrothermal treatment, annealing temperature and acid washing on the the structure and the morphology of TiO_2 nanotubes during the formation process was assessed. From EDS, XRD, SEM and TEM analysis, it can be concluded that: a) hydrothermal treatment of the TiO_2 precursor nanoparticles and the acid washing process are fundamental to form and determine the structure of nanotubes. The hydrothermal treatment modifies the crystallinity of the precursor nanoparticles, from anatase phase to monoclinic phase that characterizes the titanate nanosheets structure. The acid washing process promotes to the formation of high purity nanotubes due to Na^+ ions are exchanged from the titanate structure to the HCl solution. b) Annealing temperature influences dimensions and the morphology of nanotubes structure. Annealing temperatures in the range of 400 °C and 600 °C are optimum to maintain a highly stable tubular morphology of nanotubes. Temperatures greater than 600 °C change the morphology of nanotubes from tubular to an irregular structure of nanoparticles, which are bigger than those of the precursor material, i.e., the crystallinity changes from anatase phase to rutile phase causing the collapse of the nanotubes. c) Band gap energy of nanotubes annealed at 400 °C was similar to that of anatase phase in bulk (3.2 eV). It means that nanotubes preserved the physicochemical properties of the precursor Degussa P25 material.

Declarations

Author contribution statement

M. Á. López Zavala: Conceived and designed the experiments; Analyzed and interpreted the data; Contributed reagents, materials, analysis tools or data; Wrote the paper.

http://dx.doi.org/10.1016/j.heliyon.2017.e00456

S A. Lozano Morales: Conceived and designed the experiments; Performed the experiments; Analyzed and interpreted the data; Wrote the paper.

M. Santos Ávila: Analyzed and interpreted the data.

Funding statement

This work was supported by the National Council of Science and Technology (CONACYT) of Mexico and the Tecnológico de Monterrey.

Competing interest statement

The authors declare no conflict of interest.

Additional information

No additional information is available for this paper.

References

[1] N. Liu, X. Chen, J. Zhang, J.W. Schwank, A review on TiO2-based nanotubes synthesized via hydrothermal method: Formation mechanism, structure modification, and photocatalytic applications, Catal. Today 225 (2014) 34–51.

[2] K. Hashimoto, H. Irie, A. Fujishima, TiO2 Photocatalysis: A Historical Overview and Future Prospects, Jpn. J. Appl. Phys. 44 (2005) 8269–8285.

[3] G.K. Mor, M.A. Carvalho, O.K. Varghese, M.V. Pishko, C.A. Grimes, A room-temperature TiO2-nanotube hydrogen sensor able to self-clean photoactively from environmental contamination, J. Mater. Res. 19 (2004) 628.

[4] G. Varshney, S.R. Kanel, D.M. Kempisty, V. Varshney, A. Agrawal, E. Sahle-Demessie, M.N. Nadagouda, Nanoscale TiO2 films and their application in remediation of organic pollutants, Coord. Chem. Rev. 306 (2016) 43–64.

[5] R. Camposeco, S. Castillo, J. Navarrete, R. Gómez, Synthesis, characterization and photocatalytic activity of TiO2 nanostructures: nanotubes, nanofibers, nanowires and nanoparticles, Catal. Today 266 (2016) 90–101.

[6] A.L. Linsebigler, G. Lu, J.T. Yates Jr., Photocatalysis on TiO2 surfaces: principles, mechanisms, and selected results, Chem. Rev. 95 (1995) 735–758.

[7] Y. Lei, L.D. Zhang, G.W. Meng, G.H. Li, X.Y. Zhang, C.H. Liang, W. Chen, S.X. Wang, Preparation and photoluminescence of highly ordered TiO2 nanowire arrays, Appl. Phys. Lett. 78 (2001) 1125–1127.

 http://dx.doi.org/10.1016/j.heliyon.2017.e00456

[8] K. Varghese, D. Gong, M. Paulose, C.A. Grimes, E.C. Dickey, Crystallization and high-temperature structural stability of titanium oxide nanotube arrays, J. Mater. Res. 18 (2003) 156–165.

[9] M. Adachi, Y. Murata, I. Okada, S. Yoshikawa, Formation of Titania nanotubes and applications for dye-sensitized solar cells, J. Electrochem. Soc. 150 (2003) 488–493.

[10] T. Kasuga, M. Hiramatsu, A. Hoson, T. Sekino, K. Nihara, Formation of titanium oxide nanotubes, Langmuir 14 (1998) 3160–3163.

[11] T. Kasuga, M. Hiramatsu, A. Hoson, T. Sekino, K. Nihara, Titania nanotubes prepared by chemical processing, Adv. Mater. 11 (1999) 1307–1311.

[12] B.X. Wang, D.F. Xue, Y. Shi, F.H. Xue, Titania 1D nanostructured materials: synthesis, properties and applications, In: W.V. Prescott, A.I. Schwartz (Eds.), Nanorods, nanotubes and nanomaterials research progress, New Nova Science Publishers Inc., New York, NY, USA, 2008, pp. 163–201.

[13] K. Kiatkittipong, J. Scott, R. Amal, Hydrothermally synthesized titanate nanostructures: impact of heat treatment on particle characteristics and photocatalytic properties, ACS Appl. Mater. 3 (2011) 3988–3996.

[14] B. Vijayan, N. Dimitrijevic, T. Rajh, K.A. Gray, Effect of calcination temperature on photocatalytic reduction and oxidation of hydrothermally synthesized titania nanotubes, Jour. Phys. Chem. C 14 (30) (2010) 12994–13002.

[15] M. Mohsen Momeni, Y. Ghayeb, Z. Ghonchegi, Visible light activity of sulfur-doped TiO2 nanostructure photoelectrodes prepared by single-step electrochemical anodizing process, J. Solid State Electrochem. 19 (2015) 1359.

[16] A. Nada, Y. Moustafa, A. Hamdy, Improvement of titanium dioxide nanotubes through study washing effect on hydrothermal, Br. J. Environ. Sci. 2 (2014) 29–40.

[17] A. Le Bail, H. Duroy, J.L. Fourquet, Abinitio structure determination of LiSbWO6 by X-ray powder diffraction, Mater. Res. Bull. 23 (1988) 447–452.

[18] J. Rodríguez-Carvajal, Full Prof Suite Institute Leon Brillouin, Sclay, France, 2009.

[19] C. Legrand, J. Deville, Sur les parametres cristallins du rutile et de l'anatase, C. R. Hebd. Seances Acad. Sci. 236 (1953) 944–1946.

[20] R.J. Swope, J.R. Smyth, A.C. Larson, H in rutile-type compounds: I: Single-crystal neutron and X-ray diffraction study of H in rutile, Am. Mineral. 80 (1995) 448–453.

[21] H. Jiang, Dept of Materials Science and Engineering, Univ. of Science and Technology of China, Hefei, P.R. China, 2008.

[22] M. Wei, Y. Konishi, H. Zhou, H. Sugihara, H. Arakawa, A simple method to synthesize nanowires titanium dioxide from layered titanate particles, Chem. Phys. Lett. 400 (2004) 231–234.

[23] C.J. Brinker, G.W. Scherer, Sol-Gel Science. The physics and chemistry of sol-gel processing, Academic Press Inc., San California, USA, 1990.

[24] D.V. Bavykin, F.C. Walsh, Titanate and titania nanotubes: synthesis, properties and applications, RSC Publishing, Cambridge, UK, 2010.

[25] A. Hu, A. Apblett, Nanotechnology for water treatment and purification, Springer, Berlin, Germany, 2014.

[26] N. Harsha, K.R. Ranya, K.B. Babitha, S. Shukla, S. Biju, M.L.P. Reddy, K.G. K. Warrier, Hydrothermal processing of hydrogen titanate/anatase-titania nanotubes and their application as strong dye-adsorbents, J. Nanosci. Nanotech. 11 (2011) 1175–1187.

[27] M. Moazeni, H. Hajipour, M. Askari, M. Nusheh, Hydrothermal synthesis and characterization of titanium dioxide nanotubes as novel lithium adsorbents, Mater. Res. Bull. 61 (2014) 70–75.

[28] L.B. Arruda, C.M. Santos, M.O. Orlandi, W.H. Schreiner, P.N. Lisboa-Filho, Formation and evolution of TiO2 nanotubes in alkaline synthesis, Ceram. Int. 41 (2) (2015) 2884–2891.

[29] S.H. Cho, H.H. Nguyen, G. Gyawali, J.E. Son, T. Sekino, B. Joshi, S.H. Kim, Y.H. Jo, T.H. Kim, S.W. Lee, Effect of microwave-assisted hydrothermal process parameters on formation of different TiO2 nanostructures, Catal. Today 266 (2015) 46–52.

[30] Y.Q. Wang, G.Q. Hu, X.F. Duan, H.L. Sun, Q.K. Xue, Microstructure and formation mechanism of titanium dioxide nanotubes, Chem. Phy. Lett. 365 (2002) 427–431.

[31] G.H. Du, Q. Chen, R.C. Che, Z.Y. Yuan, L.M. Peng, Preparation and structure analysis of titanium oxide nanotubes, Appl. Phys. Lett. 79 (2001) 3702.

[32] X.M. Sun, Y.D. Li, Synthesis and characterization of ion-exchangeable titanate nanotubes, Chem. Eur. J. 9 (2003) 2229.

 http://dx.doi.org/10.1016/j.heliyon.2017.e00456

[33] D.S. Seo, J.K. Lee, H. Kim, Preparation of nanotube-shaped TiO2 powder, J. Cryst. Growth 229 (2001) 428–432.

[34] Q.H. Zhang, L. Gao, J. Sun, S. Zheng, Preparation of long TiO2 nanotubes from ultrafine rutile nanocrystals, Chem. Lett. 31 (2002) 226–227.

[35] Y. Zhu, H. Li, Y. Koltypin, Y.R. Hacohen, A. Gedanken, Sonochemical synthesis of titania whiskers and nanotubes, Chem. Commun. 24 (2001) 2616–2617.

[36] W. Mingdeng, Y. Konishi, H. Arakawa, Synthesis and characterization of nanosheet-shape titanium dioxide, J. Mater. Sci. 42 (2007) 529–533.

[37] B. Poudel, W.Z. Wang, C. Dames, J.Y. Huang, S. Kunwar, D.Z. Wang, D. Banerjee, G. Chen, Z.F. Ren, Formation of crystallized titania nanotubes and their transformation into nanowires, Nanotechnol. 16 (2005) 1935–1940.

[38] S. Sreekantan, C.W. Lai, Study on the formation and photocatalytic activity of titanate nanotubes synthesized via hydrothermal method, J. Alloys Comp. 490 (2010) 436–442.

[39] M.A. Khan, D.H. Han, O.B. Yang, Enhanced photoresponse towards visible light in Ru doped titania nanotube, Appl. Surf. Sci. 255 (2009) 3687–3690.

 http://dx.doi.org/10.1016/j.heliyon.2017.e00456